Development and calibration of a sand pluviation device for preparation of model sand bed for centrifuge tests

M. Hakhamaneshi, J.A. Black, A. Cargill, C.M. Cox & T. Elmrom
University of Sheffield, Centre for Energy & Infrastructure Ground Research, Sheffield, UK

ABSTRACT: A bespoke 0.068m^3 (18.5 gallon) sand hopper is employed at the newly established 50gTon centrifuge facility at the University of Sheffield. The sand hopper employs a series of mesh inserts of different diameters which control the flow rate and thus the relative density of the model. A series of calibration tests on equivalent Fraction E and Fraction C sands were performed to calibrate the mesh diameter and drop height for a desired relative density. Result showed that the sand hopper is capable of delivering repeatable relative densities in the range of 30% to above 90%, for both kinds of sand grades. This wide range relative density is considered sufficient to satisfy the needs of researchers preparing dry sand models for testing in the center.

1 INTRODUCTION

Many centrifuge models aim to achieve repeatable, uniform sand bed profiles of different relative densities. It is very common for researchers to develop a series of experimental parametric studies where sand beds must be uniform across the whole test series (Hakhamaneshi et al. 2015). A non-uniform relative density with a model test bed, or variations across various models, directly affects the performance of many physical model tests in the centrifuge; examples include bearing capacity footing and pile capacity tests, liquefaction and seismic site response. Many researchers also aim to compare their experimental findings with numerical predictions (e.g. Arulanandan and Scott 1993) or the experimental results to be used as a benchmark for calibration of numerical models (e.g. Hakhamaneshi et al. 2015). It is therefore essential for every centrifuge facility to employ a pourer device capable of producing repeatable uniform relative densities of a wide range that reflect loose and dense states.

Geotechnical centrifuge facilities typically employ one or more of the following sand hopper systems based on the pour area or the number of axis to be controlled (Stringer et al. 2014): point pluviators, curtain pluviators and carpet pluviators. Point pluviators pour sand typically from a small orifice where the 3-axes of pour are all controllable manually by the user. This is the most common type of placement system currently adopted in model preparation. Compared to a point pour, curtain pluviators pour a complete line of sand but need to be moved laterally to cover the entire surface area of the container in one sweeping motion. The most sophisticated pluviators cover full surface area of the model leaving the user to adjust the vertical axis during the pour (Chapman 1974)). Automatic sand pourers are also somewhat commonly used within the geotechnical centrifuge facilities. Fully robotic pourers are less common but some examples include those currently employed at the University of Cambridge, University of British Columbia, Technical University of Delft, Laboratoire Central des Ponts et Chaussees (LCPC), National Central University in Taiwan, and Hokkaido University in Japan (Chian et al. 2010). Previous studies on robotic pourers (Zhao et al. 2006) demonstrated the capability of such sand hoppers to produce uniform sand models of relative densities ranging from 50% to above 90%. Sweeney and Clough (1990) described the development of a large chamber for calibration of cone penetrometers in-situ; the chamber enabled soil pluviation for placement of sand, vacuum unit for removing the excess sand and an automatic data acquisition system.

Rad and Tumay (1987) reported the significance of pluviation intensity (mass flux) and falling height on the resulting relative density. In point pourers the mass flux is typically controlled via one or more steel mesh plates placed at the bottom end of the pourer. Rad and Tumay (1987) showed that number of identical steel mesh plates has small effects on the resulting relative density, except the case of adding a single mesh plate to a no-mesh system. In a point pourer falling sand is passed through a mesh (or a system of meshes) leading to a wider spread of area of falling sand and greater spatial uniformity

(Stringer et al. 2014, Sweeney and Clough 1990, Chapman 1974).

This paper aims to introduce the point pourer developed at the Centre for Energy and Infrastructure Ground Research (CEIGR) at the University of Sheffield. Relative density calibration charts (diameter of mesh insert and falling height) are provided for the equivalent of Fraction C and Fraction E sands.

2 SAND PROPERTIES

Two different types of silica sands named CH30 and CNHST95 were employed at the CEIGR. These sands are very similar to the commonly used Fraction C and Fraction E Leighton Buzzard silica sands (Chian et al. 2010). Table 1 summarizes the properties of the types of sands used for the pourer calibration. Figure 1 plots the Grain Size Distribution of these two types of sands.

Table 1. Properties of equivalent Fraction E and Fraction C sands used for pourer calibration.

Properties*	CH30	CNHST95
D_{10}	0.355 mm	0.100 mm
D_{50}	0.450 mm	0.139 mm
D_{60}	0.470 mm	0.150 mm
e_{min}	0.508	0.514
e_{max}	0.756	0.827
G_s	2.67	2.65

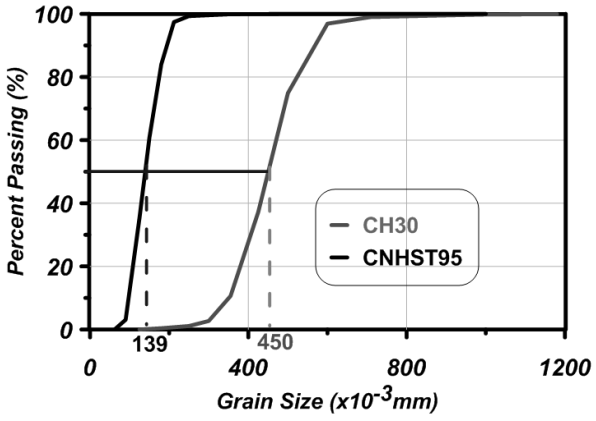

Figure 1. Grain size distribution of the equivalent Fraction C (CH30) and Fraction E (CNHST95) sands employed at CEIGR.

3 SAND PLUVIATION

3.1 *Sand pourer development*

The newly established 50gTon centrifuge facility at the University of Sheffield did not benefit from a pluviation system. A test container currently employed at CEIGR is a circular tub of 490mm diameter and 500mm height. A point sand pourer is developed which suits the current size of the container and enables a wide range of relative densities to be achieved. The system is relatively easy to operate without the need of any special training, with the exception of observing Health and Safety requirements surrounding air-borne particles. The calibration charts proposed in this paper are aimed to provide a benchmark and look up table which users can refer to determine the pluviation settings that should be observed to achieve a desired relative density.

The designed and manufactured point pourer is shown in Figures 2 and 3. The sand hopper's main body was fabricated from 2mm aluminium sheet; the four sides were cut; 380mm x 425mm and each piece was tapered and folder at a 35° angle at a distance 200mm from the top of the pourer. This angle serves to ensure that sand stored in the hopper is funnelled towards to the nozzle during pluviation to maintain a constant flow of sand.

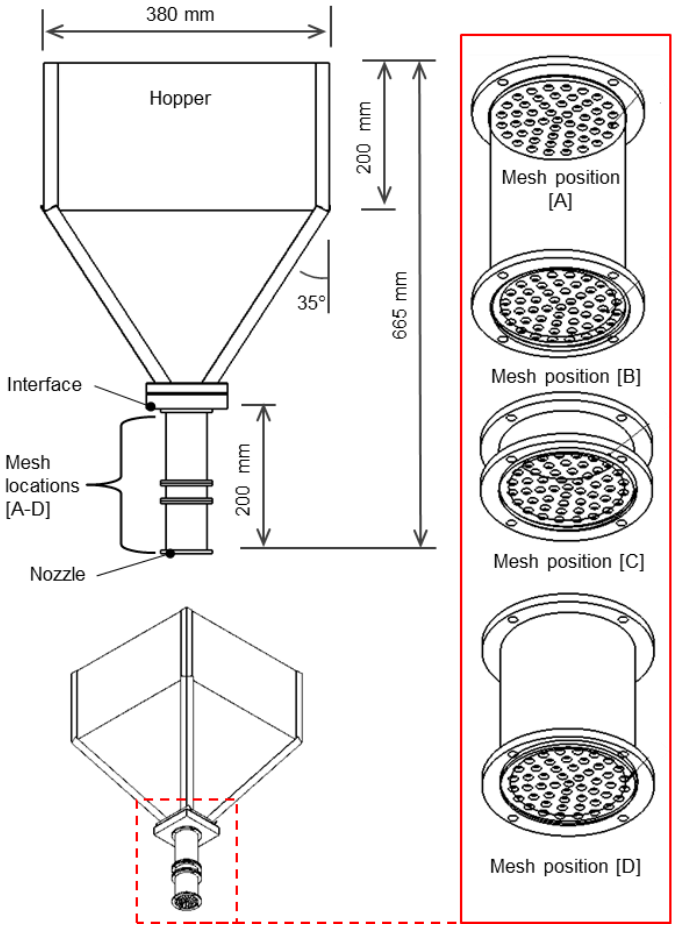

Figure 2. Schematic of the point sand pourer developed at the CEIGR along with the four allocated mesh inserts.

The hopper sides are fasted together using aluminium angle section and pop riveted to create the main pyramid shape. A base plate was fabricated at the tapered end of the hopper to interface with the end nozzle attachment. This was machined to convert the square base into a 50mm diameter outlet. The base plate was drilled and tapped to facilitate the outlet supply pipe. A length of 40mm extruded aluminium was fastened through the top of the hopper to create a lifting point so the hopper could be sus-

pended from a height adjustable pulley. This also served to strengthen the hopper overall construction. The overall capacity of the hopper is approximately $0.068m^3$.

The outlet pipe was manufactured from solid 80mm aluminium bar and consisted of 3 segmented sections and an end cap. A 50mm hole was machined through each section to correspond with the outlet from the main body. Each segment was recessed to allow a mesh filter to be inserted. Individual mesh filters were manufactured from 1 mm thick aluminium disks measuring 50mm diameter that were perforated with holes ranging from 1.5mm to 6mm. Note, the mesh reference number refers to the size of the perforations, i.e. mesh 4 has holes 4mm in diameter. It should also be noted that the mesh density decreased as the mesh diameter increased; the 1.5mm disk had a mesh density of 0.15 hole/mm^2 while the 6mm disk had a mesh density of 0.02 hole/mm^2.

The segmented system allowed the use of up to 4 mesh filters simultaneously which offers great scope to achieve various sand densities during pluviation. For reference the mesh positions are referred to as 'A to D', with 'A' being the uppermost mesh closest to the hopper body and 'D' being the mesh at the exit position. Note, a combination of meshes are denoted in sequence; i.e. Mesh 6/-/-/2 indicates mesh sizes 6 and 2 are located in position A and D respectively, with position B and C having not mesh present.

As it will be shown later, this combination of mesh possibilities enabled a wide range of mass flux and relative densities to be achieved since they could be mounted in any combination. In this paper a number of mesh combinations are evaluated to demonstrate the variations in density that could be achieved.

3.2 *Flow rate calibration*

A series of experiments are performed to study the effect of mesh diameter and D_{50} on the resulting flow rate. In the tests presented herein position A contained Mesh 6 and mesh in position B was varied between Mesh 2, 3, 4, 5 and 6; for example, 6/2/-/- through 6/6/-/-. Using these mesh configurations, the two sands, CH30 and CNHST95 are evaluated and the results are summarized in Figure 4.

Zhao et al. (2006) and Chian et al. (2010) showed that larger nozzle diameters resulted in a steep increase in the flow rate. However, an aspect not considered in their investigation was the effect of fullness of the sand pourer on the outcome. It seems reasonable to think that a fuller container might lead to a smaller flow rate due to increased arching stresses in the sand particles across perforations of the outlet mesh. The current test series investigates the effect of fullness of the sand pourer when it is completely full compared to when it is only a third full.

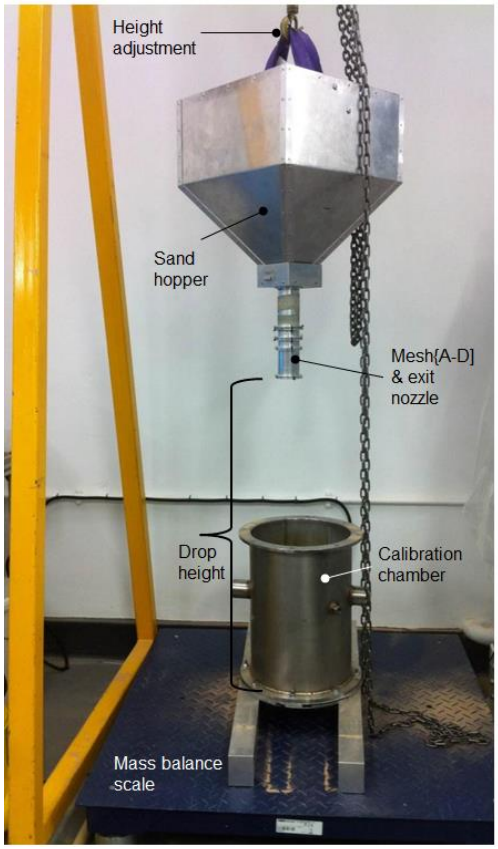

Figure 3. Sand pluviation configuration.

As shown in Figure 4, as diameter of the exit mesh increases, the flow rate increases accordingly for both types of sand. This is reasonable since at mesh perforation diameters larger than the grading of the sand, sand particles would flow more freely through the mesh resulting in flows that would be very similar thus making the effect of mesh diameter insignificant. This behaviour is visible in Figure 4 for mesh configurations greater than 6/4/-/-.

The finer sand (CNHST95) consistently has larger flow rate than the coarser sand (CH30). Finer sand particles can exit a certain mesh diameter faster than a coarser particle leading to a larger flow rate. However, the difference is less pronounced at larger mesh diameters (larger than 4mm in current study). Chian et al. (2010) also observed a similar pattern.

Also shown in Figure 4 is that the fine CNHST95 sand yields a smaller flow rate at the smallest mesh diameters (i.e. 6/2/-/- and 6/1.5/-/-) when the container is full compared to when it is a third full (due to arching). As mesh diameter increases, the difference between the two scenarios diminishes and the flow rate is dominated by the mesh diameter and not the fullness of the sand pourer. The coarser CH30 sand however does not show a significant difference between the two scenarios for any mesh diameter and the flow rate response is completely dominated by the mesh diameter and not the fullness of the container.

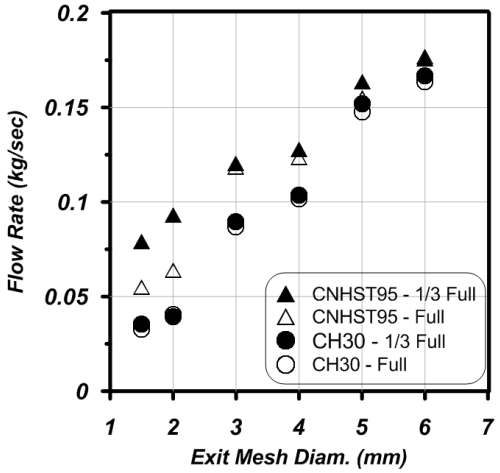

Figure 4. Effect of mesh diameter, D_{50} and fullness of sand pourer on the flow rate of the sand particles.

3.3 *Sand pourer calibration test*

A small cylindrical metal chamber of internal geometry 265mm diameter by 400mm high was used as a fixed volume standardized tub for the purpose of calibrating the sand pluviation system. This was achieved by measuring the mass of sand collected in the tub for different falling height and mesh diameter configurations.

Table 2 summarizes the implemented test matrix for calibration of the sand pourer. Test ID outlines the type of sand and diameter of the meshes used in the location of the hopper. The exit mesh in position B was varied between 1.5mm and 5mm while the mesh in position A was maintained as 6mm in diameter. The drop height was varied between 500mm and 900mm in most cases. A drop height of 1500mm was implemented for the CNHST95 sand to ensure a high relative density was achieved, as discussed in the next section. At the time of testing, the falling height was determined from the exit mesh position (i.e. mesh location B) to level of the soil surface. The height was manually kept constant during the pluviation to ensure a uniform relative density throughout the sample was achieved. An end cap was placed at the bottom of Mesh D to enable start/stop of the sand flow; to start the pluviation, the end cap was removed and a separate container was used to collect the sand being suddenly dropped from the exit mesh. Upon achieving a steady flow of sand particles, the extra container was removed to start the sand placement. During pluviation the nozzle was rotated slowly to cover the entire area of the calibration chamber. Classical sand pourers (Rad and Tumay 1987, Chapman 1974, Sweeney and Clough 1990) employ a vertical translation pluviation system only; in such systems the diameter of the nozzle is generally close in size to the size of the specimen. Due to the relatively small diameter of the nozzle of the proposed system compared to the diameter of the larger container (500mm), the sand pourer system will also benefit from a lateral translation system, using rollers on the top of the A-frame supporting the sand pourer. The translation was not necessary for the calibration tests.

A sand height of 300mm was poured in three equal height lifts for all tests detailed in Table 2. In each lift, the sand was poured above the desired lift height (100mm) and the excess sand was then vacuumed using a dual-axis height controlled vacuum system to ensure a uniform surface is achieved in each lift. The relative density for each lift was further calculated and average values are reported in this paper. If the offset relative density of any of the three layers exceeded a value of 5% from the average relative density (e.g. D_r of layer 1 being 82% while average D_r being 88%), the test was repeated to ensure a homogenous relative density across the profile of the sample was achieved.

Table 2. Sand pourer calibration test matrix.

Test ID	Drop Height	Mesh 1	Mesh 2
	mm	mm	mm
CH30_6/2/-/-	500-900	6	2
CH30_6/3/-/-	500-900	6	2
CH30_6/4/-/-	500-900	6	2
CH30_6/5/-/-	500-900	6	2
CNHST_6/1.5/-/-	500-1500	6	1.5
CNHST_6/2/-/-	500-900	6	2
CNHST_6/3/-/-	500-900	6	3
CNHST_6/4/-/-	500-900	6	4
CNHST_6/5/-/-	500-900	6	5

3.4 *Calibration test results*

The results of the tests outlined in Table 2 (except the CNHST_6/1.5/-/- test) are summarized in Figure 5 where the achieved relative densities are plotted against the corresponding drop height. The label on each plot (e.g. 6/2/-/-) outlines the mesh combination presented. For the case of the coarser CH30 sand, a wide range of relative densities (35% to 95%) was achieved for different mesh combinations. As mesh diameter increased, the achieved relative density for a constant drop height reduced. Also, as drop height increased for each mesh configuration, increases in relative density where observed. This demonstrates the significance of the secondary effect of drop height on relative density. This is consistent to results reported by Chian et al. (2010) and Zhao et al. (2006) for sands of similar D_{50} as CH30 (0.45mm).

Evident in Figure 5 is that the effect of mesh diameter (>2mm) had less pronounced effect (about 20% change) on relative density observed for the finer CNHST95 sand compared to the CH30 sand. The achievable relative density is therefore highly influenced by the very small D_{50} (Fraction E) of the CNHST95 sand and exit mesh sizes of 2mm and greater (6/2/-/- to 6/5/-/-) do not impact the achieved relative density significantly. The ratio of mesh di-

ameter to the D_{50} is therefore too large to impact the achieved relative density. As the drop height increased in the range of 500-900mm some increases in relative density of CNHST95 sand were recorded, although not at the same rate as CH30. Generally speaking while some smaller increases were observed for CH30 over the range of variables tested, the maximum achievable relative density was never greater than 50%. In order to consolidate the data into a quick look up reference chart, the results from CH30 are compiled into a solitary plot (Figure 6). The graph serves as a useful reference lookup chart whereby user can easily cross reference a desired sample density with suitable sand hopper mesh configurations and drop height.

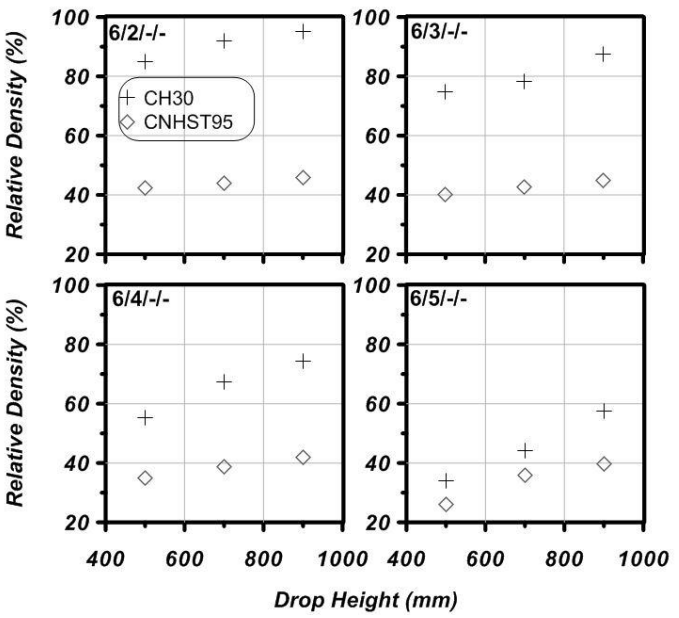

Figure 5. Effect of drop height and mesh diameter on the resulting relative density.

Evident in Figure 6 is that some overlap existing for the input variables and the output relative density. For example, if a researcher was seeking a target density of 85%, this could be achieved by mesh combination 6/3/-/- at a drop height of 50mm or by using mesh combination 6/4/-/- at a higher drop height of 900mm. A series of similar deign curves have been generated for the full range of mesh combinations.

The results from the 6/1.5/-/- mesh combination used for the finer CNHST95 sand are plotted in Figure 7. As shown, a larger range of relative densities is achieved (between 65% and 92%) but the drop height had to be increased to 1500mm to achieve a relative density above 90%.The impact of drop height on the relative density is more pronounced than the cases shown in Figure 5. Chian et al. (2010) also reported similar impact where the drop height for the fine Fraction E sand had a larger impact on the achieved density than the coarser sand. They also reported the variation of the drop height impact on the relative density with the nozzle diameter; smaller nozzle diameters led to a larger change in relative density with variation of drop height.

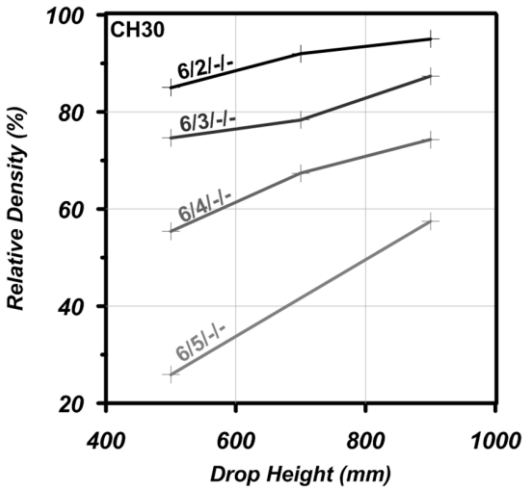

Figure 6. Relative density lookup chart for hopper input variables for CH30 sand.

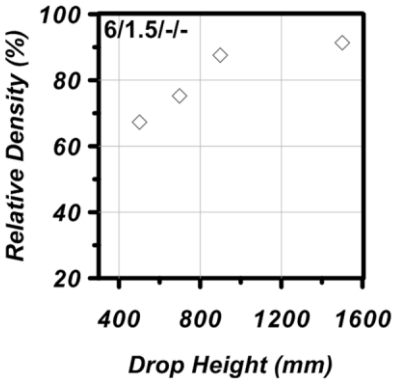

Figure 7. Effect of drop height on the relative density for the 6-1.5mm mesh for the fine CNHST95 sand.

3.5 *Theoretical fall velocity*

Chapra (2005) and Chian et al. (2010) proposed equations for theoretical fall velocity of a sand particle (Equations 1 &2) with respect to the drop height (H). A lower drop height leads to a small fall velocity which further leads to a loosely packed particle arrangement. Equation 1 shows the theoretical fall velocity (ν) of a sand particle of mass (m) with projected area of (A) falling from height of (H) in air during the elapsed fall time of (t); ρ is therefore density of air and C_d is the drag coefficient in air taken as 0.47.

$$\nu = \sqrt{\frac{m \cdot g}{\rho \cdot A \cdot C_d}} \cdot \tanh\left(\frac{t}{\sqrt{\frac{m}{\rho \cdot g \cdot A \cdot C_d}}} \right) \quad (1)$$

The elapsed fall time can further be calculated from Equation 2 below for a specific drop height (H). It should be noted that *tanh* and *arccosh* are the

hyperbolic tangent and inverse hyperbolic cosine accordingly.

$$t = \sqrt{\frac{m}{\rho \cdot g \cdot A \cdot C_d}} \cdot \operatorname{arccosh}\left(e^{\frac{H \cdot \rho \cdot g \cdot C_d}{m}} \right) \quad (2)$$

Terminal velocity (maximum attainable velocity) will be achieved when the sum of all upward forces (drag and buoyancy forces) equilibrate the downward force of gravity; the sand grain will therefore have zero acceleration at the terminal velocity. Equation 3 can therefore be derived for the terminal velocity of a sand grain.

$$v_{term} = \sqrt{\frac{2m \cdot g}{\rho \cdot A \cdot C_d}} \quad (3)$$

Figure 8 plots the theoretical fall velocity for the CH30 and CNHST95 sands with respect to the drop heights. Since the drop heights were relatively small, the terminal velocity was not achieved in either of the sands. As expected from Equations 1-3, the fall velocity and terminal velocity of the finer CNHST95 (smaller grain size) are smaller than those of the coarser CH30 sand. This pattern was also reported by Chian et al. (2010) where the fall velocity of the Fraction E sand was smaller than the velocity of the coarser sand. Chian et al. (2010) also noted that the terminal velocity was not achieved due to the low drop height.

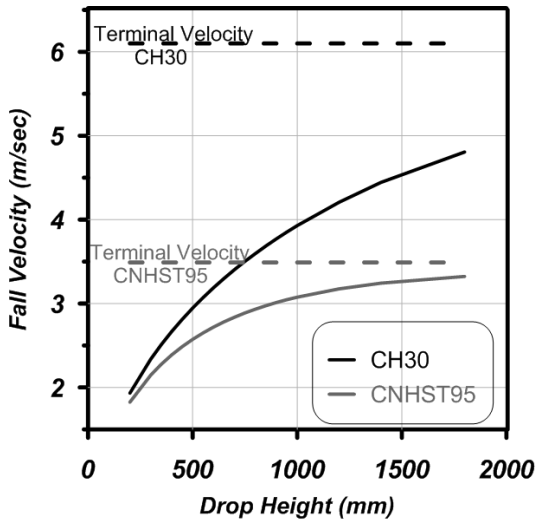

Figure 8. Variation of theoretical fall velocity with drop height.

4 CONCLUSIONS

A point sand pourer is designed and calibrated at the Centre for Energy and Infrastructure Ground Research at the University of Sheffield. The pourer was designed such that 4 mesh inserts could be used simultaneously. Effect of pour height and mesh diameter is studied to calibrate the sand hopper for different desired relative densities. Fullness of the sand hopper is also realized to impact the flow rate, a factor not previously examined in sand hopper development or sand pluviation calibration.

5 ACKNOWLEDGEMENTS

The authors would like to acknowledge the contribution by the Department of Civil & Structural Engineering technical staff for in-house technical support. Funding support provided by the Engineering Physical Sciences Research Council (EPSRC) to establish the 4 m diameter beam centrifuge and Centre for Energy and Infrastructure Ground Research at the University of Sheffield is gratefully acknowledged (EP/K040316/1).

6 REFERENCES

Arulanandan, K. & Scott, R.F. 1993. Verification of numerical procedures for the analysis of soil liquefaction problems: *Technical Papers and Discussions*, Volume 1-2. Rotterdam: A.A. Balkema.

Chapman G. A. 1974 A calibration chamber for field test equipment. *Proceedings of the 2nd European Symposium on Penetration Testing*, Stockholm, 59–65.

Chian, SC and Stringer, ME and Madabhushi, SPG, 2010. Use of automatic sand pourers for loose sand models. *Physical Modelling in Geotechnics - Proceedings of the 7th International Conference on Physical Modelling in Geotechnics*, ICPMG 2010, 1. 117-121.

Hakhamaneshi, M., Kutter, B.L., Moore, M. & Champion, C., 2015. Validation of ASCE 41-13 modeling parameters and acceptance criteria for rocking shallow foundations. *Earthquake Spectra*. (in-press)

Garnier, J., Gaudin, C., Springman, S.M., Culligan, P.J., Goodings, D., Konig, D., Kutter, B.L., Philips, R., Randolph, M.F., & Thorel, L., 2007. Catalogue of scaling laws and similitude questions in geotechnical centrifuge modelling. *International Journal of Physical Modelling in Geotechnics.*

Rad, N. & Tumay, M. 1987. Factors affecting sand specimen preparation by raining. *Geotechnical Testing Journal* 10(1), 31-37.

Stringer, M.E., Pedersen, L., Nuss, B.D. & Wilson, D.W. 2014 Design and use of a rotating spiral pluviator for creating large sand models. *Physical Modelling in Geotechnics – Proceedings of the 8th International Conference on Physical Modelling in Geotechnics 2014*, Perth, Australlia.

Sweeney B. P. and Clough G. W. 1990 Design of a large calibration chamber. *Geotechnical Testing Journal*, 13, No. 1, 36– 44.

Zhao, Y., K. Gafar, M.Z.E.B. Elshafie, A.D. Deeks, J.A. Knappett, & S.P.G. Madabhushi. 2006. Calibration and use of a new automatic sand pourer. In. C.W.W. Ng, L.M. Zhang, and Y.H. Wang (Eds.), *Physical Modelling in Geotechnics – 6th ICPMG '06*, Volume I, Hong Kong, pp. 265-270. Taylor & Francis Ltd.